ORIGINAL SCIENTIFIC PAPER

CROATICA CHEMICA ACTA

Croat. Chem. Acta **2025**, *98*(3), 207–214
Published online: June 28, 2025
DOI: 10.5562/cca4081

HKD 1926

Kinetics and Equilibrium of Methylene Blue Removal by Adsorbents Derived from Banana Peel

Pua Eng Hock, Fadina Amran, Agus Arsad, Muhammad Abbas Ahmad Zaini*

Universiti Teknologi Malaysia, Faculty of Chemical & Energy Engineering, 81310 UTM Johor Bahru, Johor, Malaysia

* Corresponding author's e-mail address: abbas@cheme.utm.my

RECEIVED: March 06, 2024 ✶ REVISED: August 09, 2024 ✶ ACCEPTED: August 12, 2024

Abstract: In this work, banana peel was transformed into hydrochar (R0A), chars (BP250 and BP600), activated carbons (R2.0. R2.5 and R3.0) and hydrochar activated carbon (R2.5A). The banana peel adsorbents were characterized for specific area, surface functionalities, morphology, surface composition and pH at point of zero charge (pH_{PZC}). The performance of adsorbents was assessed by methylene blue adsorption at different concentrations and contact times. The result shows that the R2.5 with specific area of 897 $m^2\ g^{-1}$ yields a greater methylene blue capacity of 523 mg g^{-1}. The experimental data obeyed pseudo–second order and Langmuir models, elucidating the monolayer accumulation of methylene blue molecules onto homogeneous adsorbent surface. It can be concluded that banana peel could be potentially valorized as effective adsorbent for environmental protection.

Keywords: adsorbent, adsorption, banana peel, methylene blue, phosphoric acid activation.

INTRODUCTION

The toxic effects of dye on aquatic ecosystem, food chain, and human health have long become a subject of growing concern. Dye–containing effluent from textile-related industries is less biodegradable, highly soluble and can accumulate in living tissues. Soltanian et al.[1] reported the immunosuppressive effects and potential harm to health of methylene blue dye that significantly reduces the levels of aspartate aminotransferase and neutrophils in goldfish. The continuous exposure to dye also affects the growth and reproduction of zooplankton.[2] Thus, it is of utmost importance that dye effluent must be treated before it reaches the streams.

Adsorption is a process whereby the target solute is attracted on the surface of solid adsorbent via several synergistic mechanisms.[3] It has been acknowledged as among the competitive methods to treat dye wastewater because of the straightforward operation, cheap maintenance and easy to scale–up.[4] In adsorption, the most widely used adsorbent material is activated carbon. However, the cost of commercial activated carbon is expensive due to its non–renewable feedstocks.

The price of coal–based activated carbon, for example, is USD 500 – 2000 / metric ton. The continuous demand for activated carbon has driven the quest for economical and sustainable feedstocks to manufacture activated carbon.[5] A promising candidate within this category is banana peel.

Banana peel, a waste material from banana chips factory, is freely available and abundant as feedstock of low–cost activated carbon. In Central and Latin America, for example, the annual production of banana peel is 41.3 million ton.[6] Thus, it comes with a vast opportunity in capitalizing the resource towards sustainable environment. Banana peel is generally composed of lignin, pectin, cellulose, hemicellulose, fiber and proteins, making it a potential raw material for activated carbon.[7]

The aim of this work is to expand the research horizon on the exploitation of banana peel into adsorbents for environmental protection. The adsorbents, namely char, hydrochar, activated carbon and hydrochar activated carbon were synthesized for dye adsorption from water. Methylene blue, a commonly used dye in textile industry was used as simulated pollutant to establish the governing mechanisms and performance of banana peel adsorbents.

The adsorption data were analyzed and discussed to shed insight into industrial applications. The valorization of banana peel as dye adsorbent shall enrich the field of waste and environmental management.

MATERIALS AND METHODS

Materials

Banana peel was supplied by local factory in Malaysia. Methylene blue and phosphoric acid were purchased from QReC (Malaysia). All chemicals are reagent grade and were used as received.

Preparation and Characterization of Adsorbents

Different adsorbents, i.e., char, hydrochar, activated carbon and hydrochar activated carbon were prepared from banana peel. To produce char, the dried peel was heated in a furnace at 250 °C and 600 °C for 2 h. The products were labelled as BP250 and BP600, respectively. The hydrochar (labelled as R0A) was prepared by hydrothermal carbonization using a Teflon autoclave at 170 °C for 24 h.[8] To produce activated carbon, the dried peel was mixed with phosphoric acid at weight ratios (H_3PO_4 : banana peel) of 2.0 to 3.0. The impregnated samples were pyrolyzed at 600 °C for 2 h under air–tight condition to activate the carbon surface. The activated products were labelled as R2.0 to R3.0, respectively. Lastly, the hydrochar activated carbon (labelled as R2.5A) was prepared by impregnating R0A with phosphoric acid at ratio of 2.5, followed by activation at 600 °C for 2 h.[8] The resultant samples were washed and rinsed with distilled water to a natural pH, and oven–dried prior to use.

The textural properties of adsorbents were determined using a Micromeritics ASAP–2020 at liquid N2 temperature of 77 K. The FTIR instrument (model Shimadzu IR Tracer–100) was used to obtain peaks that are attributed to specific functional groups at wavenumber ranging from 4000 to 400 cm^{-1}.

The morphology and surface composition were obtained using a field emission scanning electron microscope (FESEM Hitachi SU8020) together with EDX (Bruker XFlash 6/60 detector). All adsorbents are in powdery form, wherein the particle size can be estimated from SEM image. Meanwhile, the average pore radius of adsorbent was determined from BET analysis.

The pH of the point of zero charge (pH_{PZC}) was measured by pH drift method. First, the initial pH of 0.1 M NaCl solution, ranging from pH 2 to 11 was adjusted by few drops of 0.1 M NaOH and 0.1 M HCl. Next, 50 mg of adsorbent was added and the mixture was allowed to reach equilibrium for 24 h. The pH_{PZC} is the point where the equilibrium pH is equal to initial pH.

Adsorption studies

The calibration standard was constructed from dye solution with known concentrations (0 mg L^{-1} to 25 mg L^{-1}) based on standard visual evaluation protocols by considering level of detection (LOD) and level of quantification (LOQ) with suitable precision and accuracy (95 % probability of obtaining a correct result) using a visible spectrophotometer (model SpectrumLab 752 Pro) at wavelength of 590 nm (R^2 = 0.99). The quality assurance (QA) was established from the use replicate measurements of calibration standards.

The effect of contact time was performed to determine the rate constant, equilibrium capacity of adsorbent and time taken to attain the equilibrium point. A 30 mg of adsorbent was brought into contact with 30 mL of methylene blue solution with concentration of 100 mg L^{-1}. The residual concentrations at pre–set time intervals up to 8000 min were measured using a visible spectrophotometer. Dilution of the solution was made to bring down the concentration to a quantifiable limit. The adsorption rate at time, t was calculated as,

$$Q_t = \frac{V(C_0 - C_t)}{m} \quad (1)$$

where, Q_t (mg g^{-1}) is the dye capacity at time t, C_o, and C_t (mg L^{-1}) are the initial concentration and concentration at time t, respectively, m (g) is the adsorbent mass and V (L) is the volume of dye solution. The rate of adsorption was analyzed using pseudo–first–order, pseudo–second–order, intraparticle diffusion and Boyd's models as given in Equations (2), (3), (4), and (5–7), respectively.

$$Q_t = Q_e\left[1 - e^{(-k_1 t)}\right] \quad (2)$$

$$Q_t = \frac{k_2 Q_e^2 t}{(1 + k_2 Q_e t)} \quad (3)$$

$$Q_t = k_d t^{0.5} + C \quad (4)$$

$$B_t = -0.4977 - \ln(1 - F) \quad for\ F > 0.85 \quad (5)$$

$$B_t = \left(\sqrt{\pi} - \sqrt{\pi - \left(\frac{\pi^2 F}{3}\right)}\right)^2 \quad for\ F < 0.85 \quad (6)$$

$$F = \frac{Q_t}{Q_e} \quad (7)$$

where, k_1 (min^{-1}) is the rate constant of pseudo–first–order, k_2 (g mg.min^{-1}) is the rate constant of pseudo–second–order, k_d (mg g.min^{-1}) is the rate constant

of intraparticle diffusion and C (mg g^{-1}) is the thickness of boundary layer in intraparticle diffusion, B_t is the numerical function of Boyd's model, and F is the fraction of solute adsorbed at any time, t.

To obtain the equilibrium curve and maximum capacity, a 30 mg of adsorbent was brought into contact with 30 mL of methylene blue solution of known concentrations. Different batches of methylene blue solution at varying concentrations ranging from 5 mg L^{-1} to 1000 mg L^{-1} were prepared. The mixture was allowed to equilibrate at room temperature for 72 h. The residual concentration was measured using a visible spectrophotometer. The equilibrium capacity, Q_e (mg g^{-1}) was calculated as,

$$Q_e = \frac{V(C_0 - C_e)}{m} \tag{8}$$

where, C_e (mg L^{-1}) is the equilibrium concentration. The isotherm was analyzed using Langmuir, Freundlich, Redlich–Peterson, and Dubinin–Radushkevich models as expressed in Equations (9), (10), (11) and (12), respectively.

$$Q_e = \frac{Q_m b C_e}{(1 + bC_e)} \tag{9}$$

$$Q_e = K_f C_e^{1/n} \tag{10}$$

$$Q_e = \frac{K_R C_e}{(1 + \alpha_R C_e^g)} \tag{11}$$

$$\ln Q_e = \ln Q_D - B_D \left[RT \ln\left(1 + \frac{1}{C_e} \right) \right]^2 \tag{12}$$

where Q_m (mg g^{-1}) is the maximum dye capacity, b (L mg^{-1}) is the site binding affinity, n and K_f (mg g^{-1})(L mg^{-1})$^{1/n}$ are the Freundlich constants related intensity and capacity, respectively, K_R (L g^{-1}) and a_R are Redlich–Peterson constants, and g exponent falls between zero and unity, B_D (mol^2 J^{-2}) is the mean free energy, Q_D (mg g^{-1}) is the theoretical saturation capacity, R (8.314 J mol.K^{-1}) is the ideal gas constant and T (K) is the absolute temperature of dye solution. The mean free energy, E (kJ mol^{-1}) for each dye molecule lodged on the solid surface during the adsorption was calculated as,

$$E = \frac{1}{\left(2B_D \right)^{0.5}} \tag{13}$$

The constants were determined by non–linear regression using Solver add–in of MS Excel by minimizing the error to yield optimum regression coefficient.

RESULTS AND DISCUSSION

Characteristics of Adsorbents

Table 1 shows the yield and textural characteristics of banana peel adsorbents. Excessive burning–off in the presence of phosphoric acid activator at high temperature often results in pore widening, so diminishing the carbon yield. The phosphoric ions intercalate into the carbon matrix to enhance the volatilization of aliphatic and aromatic bonds that causes the loss in adsorbent mass.[9] The yield of hydrochar (R0A) is larger than that of chars (BP250 and BP600), thus elucidating the importance of hydrothermal carbonization in conserving the adsorbent mass. The hydrothermal carbonization produces carbon–rich and stable structure of hydrochar through aromatization, leading to high yield of R0A.[10] By direct phosphoric acid activation, the yield of banana peel activated carbon is ranging from 11.8 to 14.4 %, while that from hydrochar (R2.5A) is 57.1 %. On the same basis, the yield of R2.5A (24.4 %) is far better than R2.5 (12.4 %) because R0A contains partially decomposed material that helps in minimizing the weight loss during activation.

Table 1. Yield and textural properties of banana peel adsorbents.

Sample	Yield (%)	BET surface area ($m^2 g^{-1}$)	Average pore radius (nm)	Pore volume ($cm^3 g^{-1}$)	Microporosity (%)
BP250	17.7	0	0	0	0
BP600	20.9	5.0	21.0	0.0521	0
R0A	42.7	3.63	28.4	0.0515	0
R2.0	14.4	912	1.71	2.33	0
R2.5	12.4	897	1.68	1.96	0
R3.0	11.8	794	1.69	1.29	0
R2.5A	57.1	877	1.56	0.682	21.1

The specific area of activated carbons (R2.0−R3.0) and hydrochar activated carbon (R2.5A) are ranging from 794 $m^2 g^{-1}$ to 912 $m^2 g^{-1}$. They are more superior than chars (BP250 and BP600) and hydrochar (R0A) because of the activation effect by phosphoric acid. For different impregnation ratios of phosphoric acid, the surface area reaches a peak of 912 $m^2 g^{-1}$at ratio 2.0 before it subsides to 794 $m^2 g^{-1}$ with increasing ratio. It signifies that ratio 2.0 is sufficient to promote the optimum pore formation during activation. The pyrolysis at high temperature encourages the pore penetration effect and formation of irregular shaped pores with wide pore distribution to ease the diffusion and adsorption of dye molecules. Nonetheless, a more concentrated activator resulted in the collapse of pore walls, thus decreasing the specific area of activated carbon.[3] All activated carbons by direct activation are highly mesoporous (100 % mesoporosity). The R2.5 and R2.5A possess a similar specific area, but unlike the former, the latter contains small fraction of microporosity (21.1 %). For chars and hydrochar, the values of specific area are undeniably inferior due to the non−developed surface texture.[11]

Figure 1 shows the SEM images of banana peel and its derived adsorbents. The rough surface of banana peel becomes smooth upon the release of volatile matters after carbonization at 600 °C to form BP600. Consequently, the rudimentary pore openings are visible on the surface of BP600. Both R2.5 and R2.5A exhibit a dented texture with holes and splits, signifying a bigger pore volume as compared to banana peel and BP600. The porosity is developed when H_3PO_4 reacts with carbon atoms at the extended inter−layers of material matrix. Yet, R2.5A shows a more disintegrating morphology as a result of the prior hydrothermal carbonization process. Such texture encourages the activator to penetrate deeper inside the matrix, thus giving a rise to higher microporosity.

The surface composition of banana peel and its adsorbents by EDX instrument is summarized in Table 2. Banana peel with a 59.5 % carbon content is a promising feedstock for activated carbon. The surface carbon increases to 85.2 − 87.3 % as the raw lignocellulosic structures liberate volatiles and deforms into graphitic structure of activated carbon during activation. The surface potassium originally exists in banana peel increases to

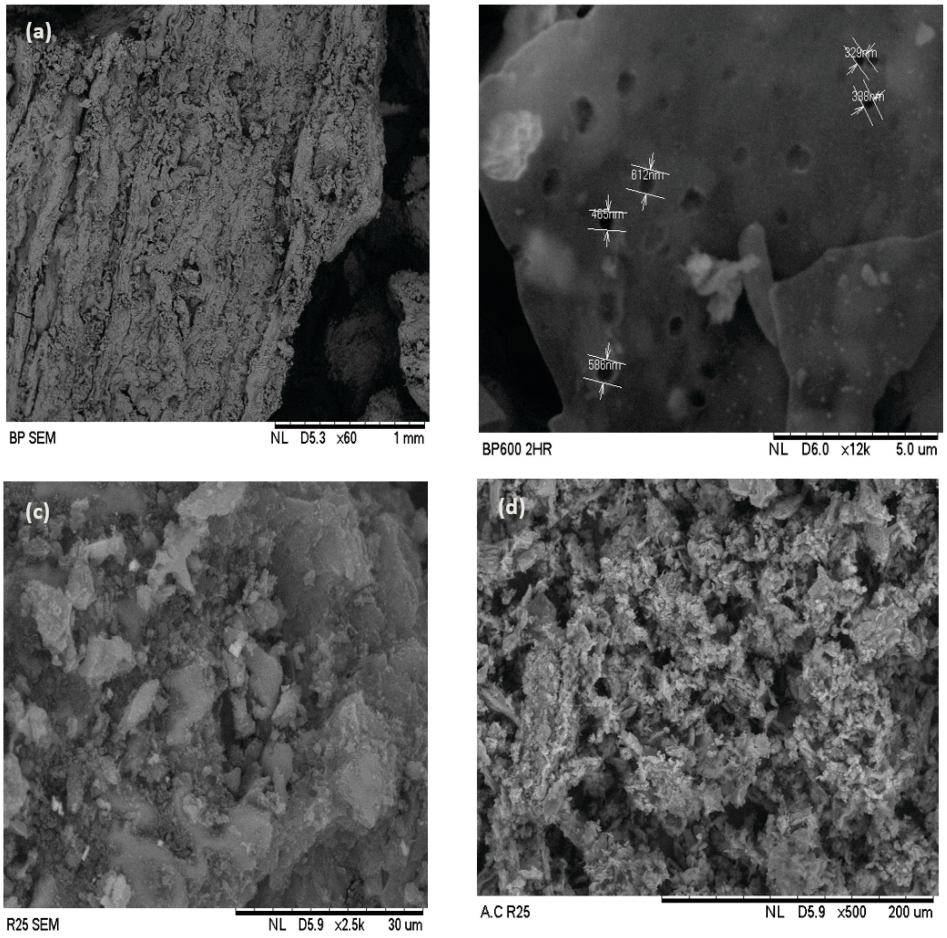

Figure 1. SEM images of (a) banana peel, (b) BP600 (c) R2.5 and (d) R2.5A.

Table 2. Surface composition of banana peel adsorbents by EDX.

Sample	C (%)	O (%)	P (%)	K (%)	Others (%)
Banana peel	59.5	35.0	0	4.06	1.44
BP600	64.1	21.0	0.4	12.7	1.80
R2.5	87.2	11.4	1.40	0	0
R2.5A	85.2	12.5	2.17	0	0.13

Values are given in mass basis.

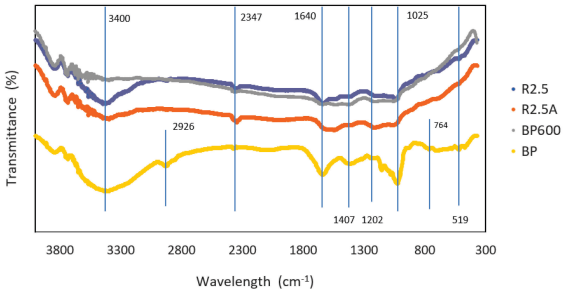

Figure 2. FTIR spectra of banana peel adsorbents.

12.7 % upon carbonization because of its higher boiling point. However, its absence in activated carbons indicates that it has been demineralized by H_3PO_4. Activated carbons also possess trace phosphorus deposit as indicated in Table 2. Phosphoric acid enhances the development of pores on the surface via the formation of phosphate bonds that widen the pore openings and intensify the surface area by connecting fragments of biopolymers (layer of carbon structure).

Figure 2 shows the FTIR spectra of banana peel adsorbents. The broad band and sharp peaks in the spectrum of banana peel (BP) are simplified after carbonization and activation. The absorption band at 3400 – 3200 cm^{-1} is generally assigned to O–H stretching vibration. The peak at 2347 cm^{-1} is the characteristic of –NH component. The peak at 1640 cm^{-1} corresponds to C=C stretching vibrations of alkenes. The peak around 1407 cm^{-1} is designated to –OH bending vibration of phenol or tertiary alcohol. The aromatic C–H in plane bending vibration is the assignment for absorption band at 1200 cm^{-1}, while the peak at 1025 cm^{-1} is associated with P–O–C stretching vibrations of aliphatic phosphates. Only the BP spectrum displays a small peak at 2926 cm^{-1} that is assigned to C–H asymmetric / symmetric stretching vibration of methylene, signifying the aliphatic chains of lignocellulosic structures.

The pH–dependent of methylene blue removal can be described according to the pH_{PZC} of adsorbent and p*K*a of dye. The pH_{PZC} of BP600, R2.5 and R.25A are 7.95, 2.95 and 3.40, respectively. The adsorbent surface becomes negatively charged when the solution pH > pH_{PZC}. As a result, the adsorption of cationic dye (e.g., methylene blue) is more facilitated towards the deprotonated surface via electrostatic attraction.[12] Meanwhile, methylene blue also holds a positive charge density with p*K*a = 3.8. For pH > p*K*a, methylene blue in the solution is cationic species.[13] The use of high temperature promotes the formation of delocalized π electrons, resulting in high basicity of material (e.g., BP600). However, it is not true for R2.5 and R.2.5A as the basic groups could be partially neutralized by phosphoric acid activator.

Adsorption Kinetics

The rate of adsorption for methylene blue was carried out at initial dye concentration of 100 mg L^{-1} and the results are shown in Figure 3. The adsorption rate, that is presented by the slope of Q_t vs. t, decreased with increasing time, to a point where the equilibrium is attained. The time taken to reach equilibrium varies depending on the number of vacant sites hold by the adsorbents studied. Usually, the more the available sites, the greater the amount of dye that can be adsorbed, thus the longer the time taken to complete the removal at equilibrium. From Figure 3, BP250, R2, R2.5, R3 and R2.5A exhibit almost 100 % removal (capacity ~ 100 mg g^{-1}) of methylene blue at C_o = 100 mg L^{-1} after 4000 min. The large surface area of

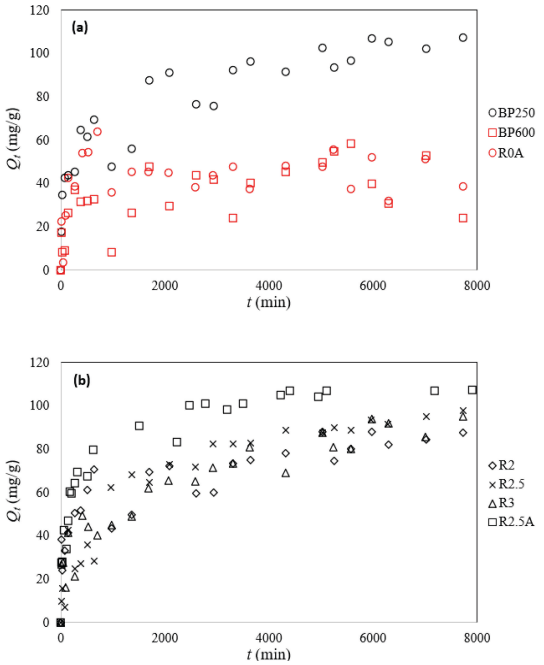

Figure 3. Rate of methylene blue adsorption by banana peel adsorbents, (a) BP250, BP600 and R0A, and (b) R2, R2.5, R2.5A and R3 at C_o =100 mg L^{-1}.

activated carbons (except BP250) provides more active sites for interaction with dye molecules, leading to high adsorption capacity. Moreover, the mesoporous texture of activated carbons encourages more interactions with dye molecules to lodge onto active sites.

Conversely, BP250, a carbon–rich char, also exhibits a similar performance with activated carbon samples. It is postulated that its surface is rich with heteroatoms, delocalized electrons and functional groups to draw more dye molecules to its surface.[14] The oxygenated functional groups with acidic properties usually exert negatively charged adsorbent surface to promote strong electrostatic attraction with positively charged (cationic) methylene blue molecules. In addition, nitrogen atoms of methylene blue may as well instigate hydrogen bonding with oxygen atoms on adsorbent surface. This explains a 100 % removal by BP250 and acceptable capacity of 55.2 mg g^{-1} by both BP600 char and R0A hydrochar. The relatively harsh heat treatment of both adsorbents when compared to BP250 expedites the release and decomposition of active sites. Consequently, a shorter period of 2000 min was taken to achieve equilibrium because of insufficient active sites. Unlike malachite green that is susceptible to form carbinol base precipitate at alkaline condition, methylene blue shows no sign of precipitation, indicating that it is chemically more stable with pH change in solution.[15]

Table 3 shows the constants of kinetic models for methylene blue removal by banana peel adsorbents. The rate of dye adsorption could be adequately described by pseudo–second–order model that offers a better fit to the experimental data than pseudo–first–order model. The applicability of this model indicates a shift mechanism that prompts the adsorption process, i.e., external diffusion at lower concentration, in which the adsorbent–phase mass transfer resistance is dominant, followed by chemical–type adsorption as concentration increases. According to Lee and Zaini,[16] this model may represent the formation of imaginary bonds due to interactions driven by electrostatic and dispersive forces.

The intensified collision among dye molecules as the concentration increases usually results in a decrease of rate constant. The rate constant, k_2 measures the reaction rate; a low k_2 represents a slow adsorption process to achieve the capacity at equilibrium. On the other hand, a rapid adsorption is depicted by a high k_2 that is likely due to more active sites and less repulsion of dye molecules.[3] Often, it is associated with high surface area and rich surface chemistry to accommodate dye molecules. Nevertheless, a high k_2 could also happen when the number of actives sites are limited, thus inducing a high concentration gradient. The BP600 and R0A exhibit faster adsorption rate because the k_2 values are higher at 1.13×10^{-4} and 4.17×10^{-4} g mg.min^{-1}, respectively.

The fast adsorption with small capacity is due to small surface area that offers restricted number of active sites. When the specific surface becomes the limiting factor, surface repulsion and active sites competition occurred, so the equilibrium could be delayed although the adsorption rate is rapid.

The pseudo kinetic models are insufficient to differentiate the effect of diffusion on adsorption. Therefore, the intraparticle diffusion model was also introduced. The constant, C is proportional to the extent of the boundary layer thickness; if the regression is close to unity and C passes through the origin, then this model is applicable to describe the transport mechanism through intraparticle diffusion. From Table 3, the regression for this model is relatively poor at $0.233 < R^2 < 0.878$ for the whole set of adsorption data although $C \rightarrow 0$. It implies that the intraparticle diffusion is not the sole rate controlling step, where some other transport mechanisms may also involve. All C values are positive, signifying a certain controlling degree of film diffusion and rapid adsorption.[16]

The Boyd's (film diffusion) model was used to shed more understanding on the mechanisms of methylene blue. Adsorption process normally consists of three sequential steps which are film diffusion (external mass transfer), particle diffusion (internal mass transport) and adsorption on the interior adsorbent surface. Dye adsorption occurs very fast inside the adsorbent matrix, so it cannot be regarded as a rate–controlling step. Thus, the adsorption can either be controlled by particle diffusion or film diffusion. The effective diffusion coefficient, D_i (cm^2 s^{-1}) for film diffusion is in the range of $10^{-6} < D_i < 10^{-8}$ cm^2 s^{-1}, while for particle diffusion, it takes the range of $10 - 11 < D_i < 10 - 13$ cm^2 s^{-1}.[16]

Equilibrium Adsorption

Figure 4 shows the equilibrium of methylene blue adsorption by selected banana peel adsorbents. The order of removal performance is given as, R2.5 (503 mg g^{-1}) > BP250 (433 mg g^{-1}) > R2.5A (337 mg g^{-1}) > BP 600 (70.1 mg g^{-1}). The R2.5 displays a greater capacity due to its

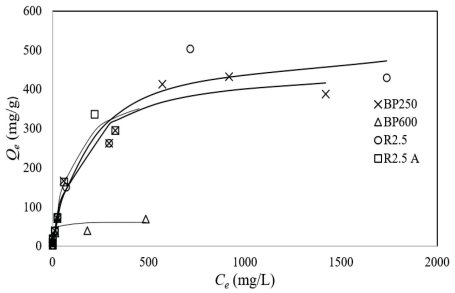

Figure 4. Equilibrium of methylene blue removal onto banana peel adsorbents (lines were predicted by Langmuir model).

Table 3. Constants of kinetic models for methylene blue removal at C_o = 100 mg L^{-1}.

Sample	$Q_{e,exp}$ (mg g^{-1})	Pseudo–first–order			Pseudo–second–order			Intraparticle diffusion			Boyd's		
		$Q_{e,cal}$ (mg g^{-1})	k_1 (min^{-1})	R^2	$Q_{e,cal}$ (mg g^{-1})	k_1 (g mg.min^{-1})	R^2	k_d	C (mg g^{-1})	R^2	B	D_i (cm^2 s^{-1})	R^2
BP250	107	101	1.55×10^{-3}	0.833	106	2.47×10^{-5}	0.884	1.06	0.001	0.779	1×10^{-5}	2.02×10^{-13}	0.908
BP600	55.2	41.9	4.44×10^{-3}	0.475	44.4	1.13×10^{-4}	0.537	0.463	0.001	0.483	6×10^{-5}	1.21×10^{-12}	0.911
R2	99.7	83.2	2.82×10^{-3}	0.695	88.8	3.94×10^{-5}	0.793	0.913	0.001	0.820	7×10^{-7}	3.79×10^{-10}	0.312
R2.5	106	98.1	7.1×10^{-4}	0.954	109	9.32×10^{-6}	0.969	0.990	0.001	0.843	4×10^{-6}	2.16×10^{-9}	0.970
R3	101	94.0	6.32×10^{-4}	0.910	103	9.87×10^{-6}	0.923	0.943	0.001	0.878	4×10^{-6}	2.16×10^{-9}	0.937
R0A	55.2	46.9	9.81×10^{-3}	0.647	47.6	4.17×10^{-4}	0.608	0.500	0.001	0.233	5×10^{-5}	2.89×10^{-11}	0.640
R2.5A	108	103	3.96×10^{-3}	0.958	106.9	1×10^{-4}	0.928	1.18	0.001	0.730	3×10^{-5}	1.74×10^{-11}	0.930

Table 4. Constants of isotherm models for methylene blue removal.

Sample	$Q_{m,exp}$ (mg g^{-1})	Langmuir			Freundlich			Redlich Peterson				Dubinin–Radushkevich		
		$Q_{m,cal}$ (mg g^{-1})	b (L mg^{-1})	R^2	n	K_f	R^2	g	K_R (L g^{-1})	a_R (L mg^{-1})	R^2	Q_D (mg g^{-1})	E (kJ mol^{-1})	R^2
BP250	433	459	0.0071	0.973	2.31	21.4	0.923	0.951	3.72	0.0115	0.973	363	28.6	0.922
BP600	70.1	61.6	0.167	0.768	4.37	17.0	0.624	1	10.3	0.167	0.768	60.2	5.43	0.786
R2	503	523	0.0053	0.955	2.63	29.9	0.902	1	2.79	0.0053	0.955	414	44.6	0.904
R2.5	337	429	0.01	0.972	1.75	12.7	0.936	1	4.28	0.01	0.972	313	23.3	0.962

high surface area and mesoporous structure. The activated carbon with high surface area offers abundant accessible sites, thus reducing the surface repulsion for greater removal capacity even at high dye concentration. The R2.5 also possesses high amount of acidic functional groups to attract methylene blue than R2.5A. The hydrogen bonding and ion–exchange mechanisms are highly connected with the oxygen–containing functional groups.[17] Moreover, the negatively charged adsorbent surface when the solution pH > pH_{PZC} can induce cationic dye molecules from the solution via electrostatic attraction.

Table 4 summarizes the isotherm constants for methylene blue removal. The Freundlich isotherm shows a poor regression in the fitting of equilibrium data, suggesting that the adsorption mechanism could not be described as the formation of multilayers of dye molecules onto heterogeneous carbon surface. The Freundlich constant, $1/n$ > 1 denotes a cooperative, multilayer adsorption, while $1/n$ < 1 reveals a close agreement to Langmuir isotherm. The n values ranging from 1.75 to 4.37 imply a standard Langmuir isotherm. In Redlich–Peterson model, $g \rightarrow 1$ shows an ideal Langmuir model. These two models supported the applicability of Langmuir isotherm ($R^2 \rightarrow 1$) to describe the adsorption mechanisms of methylene blue onto banana peel adsorbents.

The adsorption process could be described as monolayer accumulation of methylene blue molecules onto homogeneous adsorbent surface. The BP600 with high affinity (0.167 L mg^{-1}) exhibits a low maximum (Langmuir) capacity of 61.6 mg g^{-1}. It agrees well with the magnitude of rate constant, k_2 as discussed earlier. From Table 4, the Dubinin–Radushkevich model displays a comparable Q_D with experimental data and $Q_{m,cal}$ with reasonably high regression coefficient for all banana peel adsorbents studied. The E values of 44.6 kJ mol^{-1} and 23.3 kJ mol^{-1} by R2.5 and R2.5A, respectively suggest that the interactions may be driven by van der Waals force, electrostatic interaction, π–π interaction, complex formation with functional groups and mesopore filling. Therefore, the combination of physisorption and chemisorption could play a considerable role in the adsorption of methylene blue by these adsorbents.

CONCLUSION

Banana peel was converted into chars, hydrochar and activated carbons and hydrochar activated carbon for methylene blue adsorption. The R2.5 shows a greater methylene blue removal at 523 mg g^{-1} due to its high surface area and mesoporous texture. The high capacity of BP250 is reckoned through the presence of active sites to attract more dye molecules. The transport mechanism in methylene blue adsorption could be driven by particle diffusion, while the possible synergistic mechanisms include electrostatic attraction, π–π interaction, hydrogen bonding and pore filling. The valorization of banana peel is

a potent strategy to overcome environmental issues revolving its waste management and disposal. Moreover, this material could be converted into effective adsorbent for dye wastewater treatment.

Acknowledgment. Data will be made available upon request. The project was funded in part by Ministry of Higher Education Malaysia through Fundamental Research Grant Scheme No. FRGS/1/2022/STG05/UTM/02/5.

REFERENCES

[1] S. Soltanian, A. Gholamhosseini, M. Banaee, *Aquac. Res.* **2021**, *52*, 2640–2650. https://doi.org/10.1111/are.15111

[2] S. Li, Y. Cui, M. Wen, G. Ji, *Toxics* **2023**, *11*, 594–594. https://doi.org/10.3390/toxics11070594

[3] S. H. Tang, M. A. A. Zaini, *Surf. Interfaces* **2021**, *22*, 100832–100832. https://doi.org/10.1016/j.surfin.2020.100832

[4] S. Zhang, Q. Shi, C. Christodoulatos, G. Korfiatis, X. Meng, *Chem. Eng. J.* **2019**, *370*, 1262–1273. https://doi.org/10.1016/j.cej.2019.03.294

[5] A. H. Supee, M. A. A. Zaini, *Int. Wood Prod. J.* **2022**, *13*, 83–90. https://doi.org/10.1080/20426445.2021.2019175

[6] C. Redondo-Gomez, M. Rodriguez-Quesada, S. Vallejo-Astua, J. P. Murillo-Zamora, M. Lopretti, J. R. Vega-Baudrit, *Molecules* **2020**, *25*, 3829–3829. https://doi.org/10.3390/molecules25173829

[7] A. B. Guerrero, E. Munoz, *J. Clean. Prod.* **2018**, *174*, 710–717. https://doi.org/10.1016/j.jclepro.2017.10.298

[8] A. H. Supee, M. A. A. Zaini, *Biomass Conv. Bioref.* **2022**. https://doi.org/10.1007/s13399-022-03465-2

[9] M. Z. M. Nasir, G. Indiran, M. A. A. Zaini, *Part. Sci. Technol.* **2021**, *39*, 504–510. https://doi.org/10.1080/02726351.2020.1775738

[10] M. Wilk, A. Magdziarz, I. Kalemba-Rec, M. Szymanska-Chargot, *Energy* **2020**, *202*, 117717. https://doi.org/10.1016/j.energy.2020.117717

[11] N. A. Rashidi, S. Yusup, *J. Hazard. Mater.* **2021**, *403*, 123876. https://doi.org/10.1016/j.jhazmat.2020.123876

[12] G. M. Yildirim, B. Bayrak, *Biomass Conv. Bioref.* **2022**, *12*, 4785–4797. https://doi.org/10.1007/s13399-021-01501-1

[13] H. R. Sousa, L. S. Silva, P. A. A. Sousa, R. R. M. Sousa, M. G. Fonseca, J. A. Osajima, E. C. Silva-Filho, *J. Mater. Res. Technol.* **2019**, *8*, 5432–5442. https://doi.org/10.1016/j.jmrt.2019.09.011

[14] M. A. Yahya, M. H. Mansor, W. A. A. W. Zolkarnaini, N. S. Rusli, A. Aminuddin, K. Mohamad, F. A. M. Sabhan, A. A. A. Atik, L. N. Ozair, *AIP Conf. Proc.* **2018**, *1972*, 030023. https://doi.org/10.1063/1.5041244

[15] P. E. Hock, A. N. M. Faizal, L. Sirajo, M. A. A. Zaini, *Biomass Conv. Bioref.* **2023**. https://doi.org/10.1007/s13399-023-04117-9

[16] L. Z. Lee, M. A. A. Zaini, *Toxin Rev.* **2022**, *41*, 64–81. https://doi.org/10.1080/15569543.2020.1837172

[17] H. D. Nguyen, H. N. Tran, H-P. Chao, C-C. Lin, *Water* **2019**, *11*, 2581. https://doi.org/10.3390/w11122581